Journal of Nuclear Materials 429 (2012) 315–324

Contents lists available at SciVerse ScienceDirect

Journal of Nuclear Materials

journal homepage: www.elsevier.com/locate/jnucmat

Mobility and stability of large vacancy and vacancy–copper clusters in iron: An atomistic kinetic Monte Carlo study

N. Castin [a,*], M.I. Pascuet [b], L. Malerba [a]

[a] Studiecentrum voor Kernenergie – Centre d'Etudes de l'énergie Nucléaire (SCK•CEN), Nuclear Materials Science Institute, Unit Structural Materials Modelling and Microstructure–Boeretang 200, B2400 Mol, Belgium
[b] Consejo Nacional de Investigaciones Científicas y Técnicas (CONICET), Av. Rivadavia 1917, C1033AAJ Buenos Aires, Argentina

ARTICLE INFO

Article history:
Received 21 March 2012
Accepted 14 June 2012
Available online 23 June 2012

ABSTRACT

The formation of Cu-rich precipitates under irradiation is a major cause for changes in the mechanical response to load of reactor pressure vessel steels. In previous works, it has been shown that the mechanism under which precipitation occurs is governed by diffusion of vacancy–copper (VCu) complexes, also in the absence of irradiation. Coarse-grained computer models (such as object kinetic Monte Carlo) aimed at simulating irradiation processes in model alloys or steels should therefore explicitly include the mobility of Cu precipitates, as a consequence of vacancy hops at their surface. For this purpose, in this work we calculate diffusion coefficients and lifetimes for a large variety of VCu complexes. We use an innovative atomistic model, where vacancy migration energies are calculated with little approximations, taking into account all effects of static relaxation and long-range chemical interaction as predicted by an interatomic potential. Our results show that, contrary to what intuition might suggest, saturation in vacancies tend to slow down the transport of Cu atoms.

1. Introduction

Hardening and embrittlement under the effect of neutron irradiation of low alloy ferritic steels, used as structural materials for reactor pressure vessels, are limiting factors to the lifetime of existing nuclear power plants [1]. It is long established that radiation-enhanced copper precipitation is one of the major causes for these changes in mechanical response [2,3], because precipitates act as obstacles to dislocation motion. For this reason, radiation-induced copper precipitation in steels and alloys has been intensively studied in the past, both experimentally (see e.g. [4–8]), and using computer simulation. In particular, rate theory [9–12] or object kinetic Monte Carlo (OKMC) [13] approaches are tools that allow irradiation processes to be described up to large time scales, enough to cover the lifetime of reactor pressure vessel (RPV) steels, and have been used to model copper precipitation in iron under irradiation. The interested reader can find a review of these approaches in [14].

Nanostructural changes under irradiation, e.g. Cu precipitation, are enhanced by the supersaturation of point-defects that are debris of atomic collision cascades triggered by impinging high energy neutrons. In particular, vacancies have been shown to interact strongly with Cu atoms and precipitates, both experimentally and using electronic structure or interatomic potential calculations [15–19], leading to the formation of small vacancy–copper (henceforth denoted as VCu) complexes from the early stages of the irradiation (see e.g. [13]). The interaction is sufficiently strong to lead to the dragging of Cu atoms by vacancies [20–22], ending up with the formation of Cu precipitates that can efficiently trap vacancies [21,23] and may contain a significant amount of them [24,25]. The formation of vacancy clusters associated with Cu atoms under both neutron and electron irradiation has received clear experimental confirmation from positron annihilation spectroscopy [26–29]. It seems therefore established that, as put forward already in [13], the mechanism leading to Cu precipitation under irradiation is governed by the diffusion of vacancy–copper clusters.

We have recently been able to simulate successfully the complete coherent stage of copper precipitation in body-centred-cubic (bcc) iron under thermal ageing, at different temperatures and alloy compositions, using a kinetic Monte Carlo model [30]. Pivotal for the success of the model was that it explicitly included the possibility for copper precipitates to diffuse, because of the long time spent by the vacancy inside them [30], according to a mechanism proposed for the first time in [23]. This is an additional argument to suggest that the mobility of copper clusters, up to large sizes, should play a central role in the precipitation kinetics under irradiation. The mobility of VCu clusters of any size should therefore be included in relevant models, with carefully calculated parameters.

Unfortunately, the diffusion properties of VCu clusters cannot be experimentally measured, because no experimental technique allows them to be imaged and their trajectory to be followed, to

* Corresponding author.
E-mail addresses: ncastin@sckcen.be (N. Castin), pascuet@cnea.gov.ar (M.I. Pascuet).

0022-3115/$ - see front matter © 2012 Elsevier B.V. All rights reserved.
http://dx.doi.org/10.1016/j.jnucmat.2012.06.020

collect statistics about their diffusion coefficient. The mobility of these clusters is the consequence of sequences of vacancy hops at their surface. Estimates obtained analytically for large precipitates in the hypothesis that a single vacancy diffuses on their surface do not provide sufficiently reliable predictions [23] and will certainly fail for small sizes and large vacancy-to-copper ratios.

For this reason, in [22] we started a systematic study of the stability and mobility of small V_mCu_n clusters, using advanced atomistic kinetic Monte Carlo (AKMC) techniques, in which an accurate estimation of the energy migration barriers as functions of the environment is achieved by using appropriately trained neural networks [22,30,31]. The cluster was created in the simulation and allowed to diffuse as a consequence of elementary vacancy migration events, thereby taking into full account the atomistic nature of the process, differently from the case of OKMC models, where each cluster migrates as a whole with an effective migration energy. These effective values are exactly those that we can obtain with our more detailed model. In this work we extend that study to much larger cluster sizes. In order to do so, our AKMC model, or more precisely the definition of the local environment to which the neural network is trained for migration energy barrier calculations, had to be generalised to the case of environments containing any number of vacancies. The paper is organised as follows. In the first part (Section 2), we recall the essential features of our atomistic model, explaining how the algorithm is generalised to allow the introduction of many vacancies in the simulation environment. In the second part (Section 3), the newly proposed atomistic model is applied to study the mobility and stability of a large variety of VCu clusters.

2. Artificial neural network based AKMC algorithm

AKMC methods are widespread tools to study diffusion-controlled microstructural and microchemical evolution in alloys during thermal ageing and under irradiation (see e.g. [1,4,32–39]). In these models, the atoms of the alloy are located on the positions corresponding to the crystallographic structure of interest, generally on a rigid lattice. The evolution of the system is driven by the migration of point-defects, generally vacancies [1,4,32–39], whose position is exchanged with nearest neighbour atoms (migration jump) [9,39]. The jump to occur is each time selected stochastically amongst all possible ones, based on the Monte Carlo method, according to their frequencies of occurrence. The latter are calculated as thermally activated events:

$$\Gamma = \Gamma_0 \cdot \exp\left(\frac{E_m}{k_B T}\right) \tag{1}$$

where Γ_0 is the jump attempt frequency (which can be considered as a constant in first approximation), T the absolute temperature and E_m the migration energy barrier. Time is then deduced from the residence-time algorithm [40–42]. In such a model, it is clear that the reliability of the physical description of the system resides chiefly in the value of the migration energies, i.e. the way they are calculated at every step of the simulation. The fundamental assumption is that these energies are an *a priori* unknown function of the local environment (atomic species and their distribution in space). In order to approximate this function, expressions fitted to energy data from interatomic potentials or *ab initio* can be obtained using broken-bonds formalisms [23,39,43–45], cluster expansion [46,47], genetic programming [48], or other simplified approaches that make the barrier dependent on the final state [43,49–53]. In our model [22,30,31], the migration energies are calculated for a given local atomic environment (LAE) with the nudged elastic band (NEB) method, using an interatomic potential as Hamiltonian. All the effects of long-range chemical and elastic interactions, as well as static relaxation, as stemming out of the used potential, are therefore largely taken into account. However, repeating at each Monte Carlo step an NEB calculation would make the simulation extremely slow. To speed up the simulation by many orders of magnitudes, an artificial neural network (ANN) is designed to replace NEB, by being trained to predict the value of the migration energy when given as input a description of the LAE in terms of on-site variables.

This methodology, the numerical and implementation details of which are explained in [31], to which the reader is referred to has been successfully applied in [30] to the simulation of thermal annealing experiments for Fe–Cu alloys, using an interatomic potential by Pasianot et al. [54]. Our results compared very accurately to experimental measurements (for various alloy compositions and temperatures), which proves that relevant predictions for the kinetics of precipitation can be achieved, given appropriate interatomic potentials, at least in the absence of irradiation. The description of the LAE in that case was, however, relatively simple: since only one vacancy needs to be introduced in the simulation box in thermal annealing simulations, the LAE at each jump is simply described by two-value on-site variables telling whether a given lattice site is occupied by an iron or a copper atom. In order to be able to train the neural network to more complex LAEs, that include the presence of other vacancies, our algorithm needs generalisation, as described in the next sections.

2.1. Generalisation to any number of vacancies

In the single vacancy case, appropriate to simulate thermal annealing experiments, our AKMC algorithm can be genuinely seen as an acceleration of molecular dynamics (MD), in which the consequence of thermal vibrations around the equilibrium positions is described by Eq. (1). As a matter of fact, since the coefficients in Eq. (1) are calculated consistently with the same potential that would be used in MD, including relaxation, the predictions are to a good extent equivalent, although covering much longer times, so long as high-temperature vibrational entropy effects can be neglected, which is the case for the Fe–Cu system [55].

The introduction of a small number of vacancies in the LAE is formally easily achieved by simply adding a third possible value for the on-site variables, because in this limit vacancies can be simply treated as additional chemical species, that do not distort significantly the relaxed geometry of the lattice. In Ref. [22], we have already modelled in this way the migration and dissociation of very small clusters, limited to six vacancies and a few copper atoms.

Generalising our AKMC algorithm to allow any number of vacancies in the LAE to be included (Fig. 1) implies making sure that the representation of the LAE on a rigid lattice description, and the corresponding choice of the vacancy jump, is still sufficiently close to the evolution of the system as it would be described in a MD simulation of the same process. In order to achieve this goal, the following choices were made:

- For the definition of the LAE in terms of on-site variables (i.e. string of integers, e.g. 1 for Fe, 2 for Cu, 0 for vacancies) the rigid lattice description is retained for convenience. However, the exact lattice sites are replaced by Wigner–Seitz (WS) cells built around the regular lattice positions for a perfect crystal. During relaxation in the presence of a certain number of vacancies initially assigned, atoms will move off-site (MD world); however, so long as they stay within the same WS cell, they remain assigned to the corresponding lattice site (rigid lattice world), thereby defining the value of the corresponding on-site variable. An empty WS cell will be assigned the on-site variable value for the vacancy.

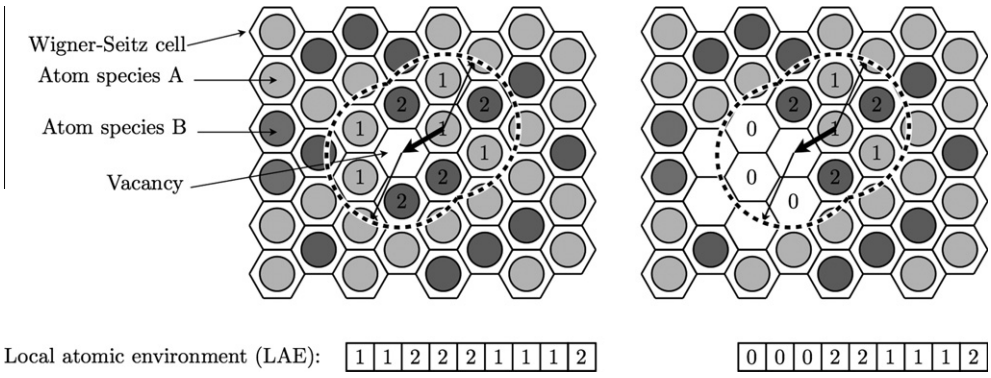

Fig. 1. Schematic illustration in 2D of the representation as a rigid lattice of the simulated crystal. The atomic volumes corresponding to lattice positions are delimited by Wigner–Seitz cells. The thick arrow shows the atomic/vacancy exchange that are being considered. The dashed lines show the definition of the LAE for that jump. (Left) Single-vacancy case. (Right) vacancy–cluster case.

- Again for convenience, the list of possible transitions for the system at every step of the simulation remains predefined. However, the jump of a vacancy to a first nearest neighbour (1nn) position is now only one of a series of possible transitions, such as the jump to a second nearest neighbour (2nn) position, or the joint migration of several vacancies at a time (Fig. 2). For every type of transition, tables of examples of energy barriers versus LAE must thus be calculated using NEB, and a specific ANN is trained to predict each of them, given as input the string of integers that describes the LAE.

The most important condition for the above choices to respect reasonably the physics of the studied system is that for any state that exists in the rigid lattice world, i.e. for any possible distribution of atoms and vacancies within the defined atomic volumes, there exists one and only one (meta)stable state of the system after static relaxation. This condition is always fulfilled in the case of single-vacancy systems, but this is *a priori* not guaranteed if many vacancies are introduced. We however checked that in practice, for the configurations studied in this work, this condition is almost always fulfilled, as will be discussed later. There is of course a risk that unrealistic paths are considered in the AKMC evolution, as illustrated in Fig. 3. This problem could be in principle tackled by redefining unrealistic transitions, after detecting unstable states on-the-fly during the simulation (see again Fig. 3). In our experience, ANN capable of detecting unstable states can be efficiently designed for this purpose. In practice, though, for the present application unstable states have been verified to be rare, so this option is not necessary. This implies that we accept the risk that, very occasionally, the transitions that we consider in the model might not be precisely those that would occur in a hypothetical MD simulation of the same system in the same situation. In all these cases the ANN will provide a barrier, i.e. from the point of view of the model it will be an event like any other. Thus, without a specific ANN recognition we cannot precisely assess how often it occurs but, based on separate analyses, we can state that these will be extremely rare events, which are not expected to impact significantly the overall results or which will simply be part of the many sources of uncertainty on the final results.

2.2. Selection of migration mechanisms to be included

The number of *a priori* possible collective migration jumps of vacancies rapidly explodes when the number of vacancies increases. Moreover, most of these transitions, as well as jumps of single vacancies to further distances than 1nn, are likely to be associated with high energy barriers, that would barely be competitive compared to transitions of single vacancies to a 1nn position. In order to avoid introducing unnecessary complexity in the model, we have estimated the potential competitiveness of events of the type (b) and (c) in Fig. 2, as predicted by the interatomic potential.

For this purpose, 100 possible atomic configurations were randomly selected for 30 different V_mCu_n clusters (3000 configurations), with $m = 6,..,10$ and $n = 2,..,10$. For each configuration, the complete list of possible events of type (a), (b) and (c) was generated and the corresponding energy barriers were calculated with the NEB method. Events (a) and (b) are easily defined, and the maximum number of these events, removing irrelevant ones where vacancies exchange their position with another vacancy, is equal to 8 times or 6 times the number of vacancies in the cluster at the most. The selection of events of type (c) was limited to no more than two migrating vacancies at a time, located at 1nn or 2nn distance from each other, and exchanging position with atoms that are either 1nn or 2nn to each other.

By calculating about 50,000 energy barriers, the relative probabilities for events of type (a), (b), or (c) in Fig. 2 could be evaluated. The conclusion was that type (a) events are clearly dominating the other ones. Type (b) events have a probability that varies between

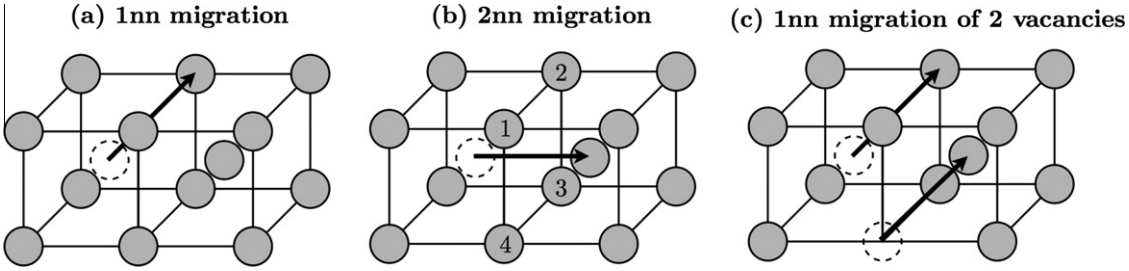

Fig. 2. Examples of vacancy jump events to be considered in AKMC simulations. (a) Jump of a single vacancy to a 1nn position. (b) Jump of a vacancy to a 2nn position. This event is only defined if at least two sites amongst those denoted as 1, 2, 3 and 4 are occupied by vacancies. (c) Joint migration of two close vacancies to a 1nn position.

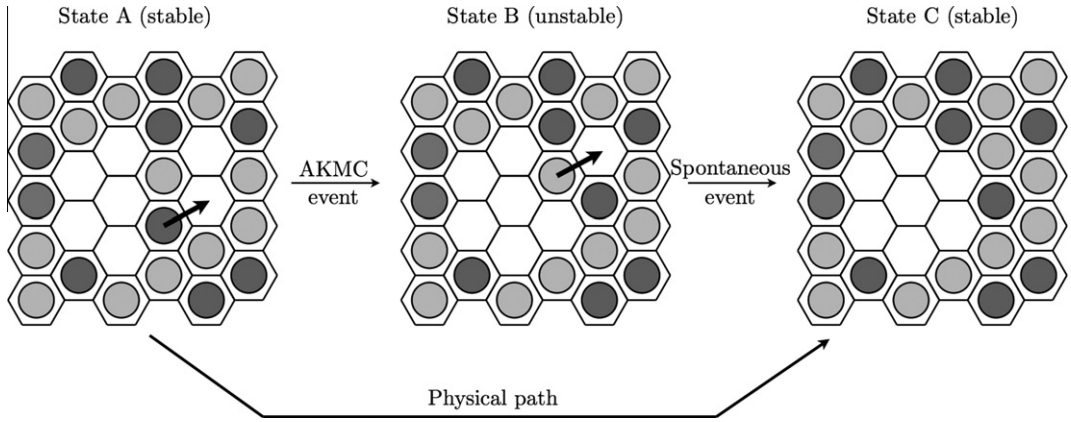

Fig. 3. Example of redefinition of events in the AKMC simulation, when necessary. The initial state A is stable, and migration to state B is amongst the list of possible events generated automatically during the simulation. With atomic relaxations, however, state B is unstable, and spontaneously evolves into state C. If this spontaneous B–C transition can be detected on-the-fly during the simulation, the A–B event can be replaced by A–C, without passing via state B.

2.5% and 15%, depending on cluster composition, whereas type (c) events are extremely rare, with a probability varying between 0.001% and 0.01%. It is therefore clear that the migration of VCu clusters is mainly driven by the migration of individual vacancies to a 1nn position, and other events can be disregarded. Migration jumps to a 2nn position can in some cases play a minor role, but are very unlikely to change the global migration properties in a significant way.

For the sake of completeness, this study on the probability of the different events has been complemented with a different approach. A few configurations were used as input for the monomer method proposed by Ramunni et al. in Ref. [56]. This method, like Henkelman's dimer [57], explores the energy landscape around a metastable state, and searches for all possible transitions towards other metastable states. This study did not reveal the existence of other highly probable transitions than 1nn jumps of individual vacancies, consistently with our previous conclusions.

2.3. Design of training examples for the ANN to predict vacancy migration energies

Consistently with the conclusions of the previous section, we trained ANNs to predict the migration energy for single vacancies to a 1nn position, the other vacancies of the system remaining immobile. The general procedure we followed to design the ANN is essentially the same as in our previous works (see detailed description of the method in [31]), but the specific choices made in this particular case are described in what follows.

First, a table of examples of LAEs is generated at random, though taking care that all types of configurations that can be encountered during the AKMC simulations are represented in equal proportion. In this respect, the most delicate point consisted in considering V_mCu_n clusters of relatively large sizes in physically relevant topologies. In Ref. [25], Al-Motasem et al. showed, with an off-lattice Metropolis Monte Carlo model and with the same potential that is used here, that in the most stable configurations vacancies form nearly-spherical clusters, the Cu atoms playing the role of coating, as shown schematically in Fig. 4 (the same result was obtained in [24], using earlier interatomic potentials). Depending on the m/n ratio, these configurations can vary from a cavity decorated by a few Cu atoms on the surface ($m/n \gg 1$), to hollow Cu precipitates with a vacancy core that does not have any contact with Fe atoms ($m/n \ll 1$). The actual configuration will no doubt influence the kinetics of migration and dissociation of these clusters. When preparing the examples of LAE for which to calculate

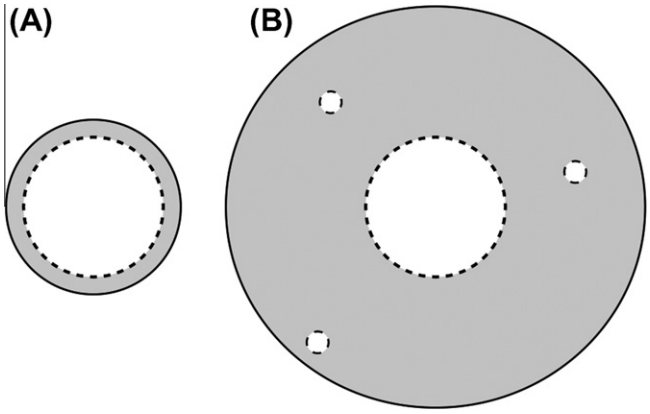

Fig. 4. Schematic representation of the different V_mCu_n clusters configurations considered to train the ANN. Dashed circles represent vacancies, and grey areas Cu atoms. (A) Vacancy cluster coated with a few Cu atoms, at the most enough to cover completely the surface of the vacancy cluster. We considered here $m = 2,\ldots,250$ and $n/m = 0,1/4,1/2,1,3$. (B) Vacancy cluster coated with a large number of Cu atoms. Most of the vacancies remain in a spherical configuration in the bulk of Cu, but a couple vacancies could escape and diffuse away. We considered here $m = 2\ldots,250$ and $n/m = 5$, 10 and 100.

the vacancy migration barrier, we have therefore explicitly considered also limiting cases, including those where a few vacancies escape the precipitate core and diffuse in bcc Cu, because this is the only way such a structure can migrate and emit vacancies or Cu atoms.

In a further step, the migration energy associated with all entries in the table of LAEs is calculated using NEB. Ref. [31] addresses clearly the problem of the convergence of the NEB prediction with the size of the LAE, so this aspect is not discussed here. The procedure is, classically: (a) initial and final states are created on a rigid lattice; (b) they are separately relaxed using a conjugate gradients method. Relaxation is actually performed several times, from different random small perturbations of the rigid lattice configuration, to investigate if distinct metastable states corresponding to the same LAE may exist according to the potential, as this would question the validity of the assumption of biunivocal correspondence between rigid lattice and relaxed configurations: it is almost never the case in practice, so the assumption is safe; (c) a first estimate of the migration path is made with a linear interpolation of all atomic positions, to create a chain of transition states; (d) the chain of states is optimised in the energy landscape, using the NEB method, until convergence. The only part of the procedure that needs special

precaution is step (b), because several vacancies are present. It is at this stage that configurations that are possible in the rigid lattice world, but are in fact unstable according to the potential, may appear. Fortunately, as mentioned, we observed that the number of unstable configurations is limited, which supports the AKMC algorithm proposed in Section 2.1. Also, instabilities never involved more than one or two vacancies. When encountered, LAEs involving instability were discarded from the table, and no migration energy was calculated. If included, they would have represented misleading points for the training of the ANN.

Additional energy barriers were computed, to complement those in Section 2.2, to collect a total number of 75,000 examples of 1nn jumps. The ANN was trained on the basis of these barriers using the gradually improving accuracy constructive algorithm described in Ref. [31], where layers of nearest neighbours (nn) around the migrating vacancy and migrating atom are progressively connected to the network. The algorithm converged after connection of the 5th nn, that represent 77 atomic sites. Comparison between the ANN prediction and migration energies is shown in Fig. 5. We see that they can be considered as reasonably accurate on the average, even though the prediction error can be as large as 200 meV in some cases. Fig. 6 shows that the error is smaller than 20 meV in about 50% of the cases, and smaller than 70 meV in 90% of the cases. ANN predictions are thus not perfect, but we consider them as acceptable, especially because there is no prediction bias. From past experience, there is no reason to believe that the precision of the ANN would improve significantly by further increasing the number of examples. In addition, we have checked that the accuracy of prediction is homogeneous for all types of LAE that was considered, and in particular it does not vary with the number of vacancies or Cu atoms in the cluster.

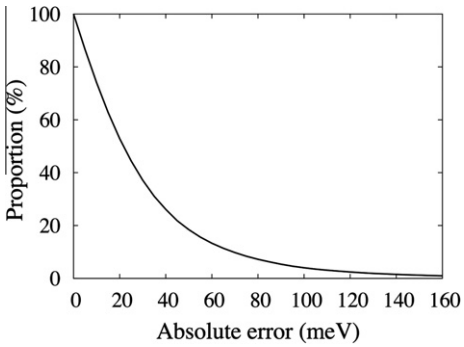

Fig. 6. Proportion (in %) of ANN predictions subjected to absolute error larger than a given value (x axis, in meV).

3. Calculation of copper–vacancy cluster diffusion coefficients and lifetimes

In this section, we use the neural network based AKMC, generalised to any number of vacancies in the LAE, as described in the previous section, to describe the kinetics of migration and dissociation of V_mCu_n clusters. Since the results are meant to be usable for example to parameterize OKMC models of radiation-enhanced Cu precipitation in Fe, we extracted information from our simulations to provide frequencies for the following events:

Migration of the cluster without dissociation. In OKMC models such as the one by Domain et al. [58], the migration of all objects can only occur, for convenience, to a 1nn position, based on a known jump frequency. In reality, not all clusters (or rather, their centre of mass) will cover this distance before dissociation. It is thus more convenient to use AKMC simulations to derive the diffusion coefficient D (using the method described in [22], see below), from which, neglecting correlations, the migration frequency to a 1nn position, Γ_{1nn}, can be deduced using the simple relation:

$$\Gamma_{1nn}(m,n,T) = D(m,n,T)/6\Delta^2 \quad (2)$$

where Δ is the 1nn distance and T is the absolute temperature.

Dissociation of the cluster by the emission of a vacancy. The associated frequency, denoted as Γ_V, can be measured directly as the inverse of the average time taken for one vacancy to escape from the cluster. The latter time is denoted as lifetime, τ_{life}, vacancy emission being the most frequent cluster dissociation mechanism. We thus write:

$$\Gamma_V(m,n,T) = 1/\tau_{life}(m,n,T) \quad (3)$$

Dissociation of the cluster by the emission of a vacancy–Cu pair. These events are quite rare, and are not easily observed during AKMC simulations. Simulations should consequently be run a very large number of times to collect enough statistics on them. Even though we did calculate the frequency of emission of VCu pairs from VCu_n clusters ($m = 1$ and $n = 20$ to 6000) in Ref. [30], we did not undertake this task in this work for $m > 1$, because of the prohibitive computing time it would require. Instead, emission frequencies can be roughly estimated, e.g. using the formulas for the binding energies derived by Al-Motasem et al. in Ref. [25].

3.1. Calculation method

Given a V_mCu_n cluster, we first create it in an AKMC simulation box, in a configuration close to the one that is assumed to be its most stable one: the m vacancies are arranged within a sphere in the centre, and the n Cu atoms are placed on its surface, equally filling the layers of close neighbours one after another, as necessary.

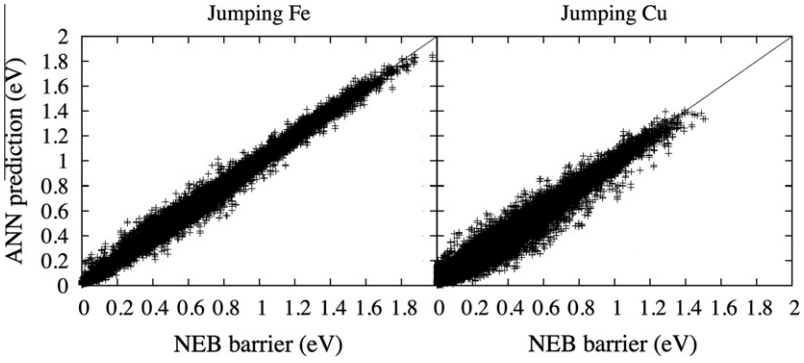

Fig. 5. Comparison between predictions of the ANN with the energy barriers calculated with NEB. (Left) Jumping Fe case: the average error is 25.5 meV, and the correlation coefficient R^2 is 0.995. (Right) Jumping Cu case: the average error is 35.2 meV, and the correlation coefficient R^2 is 0.985.

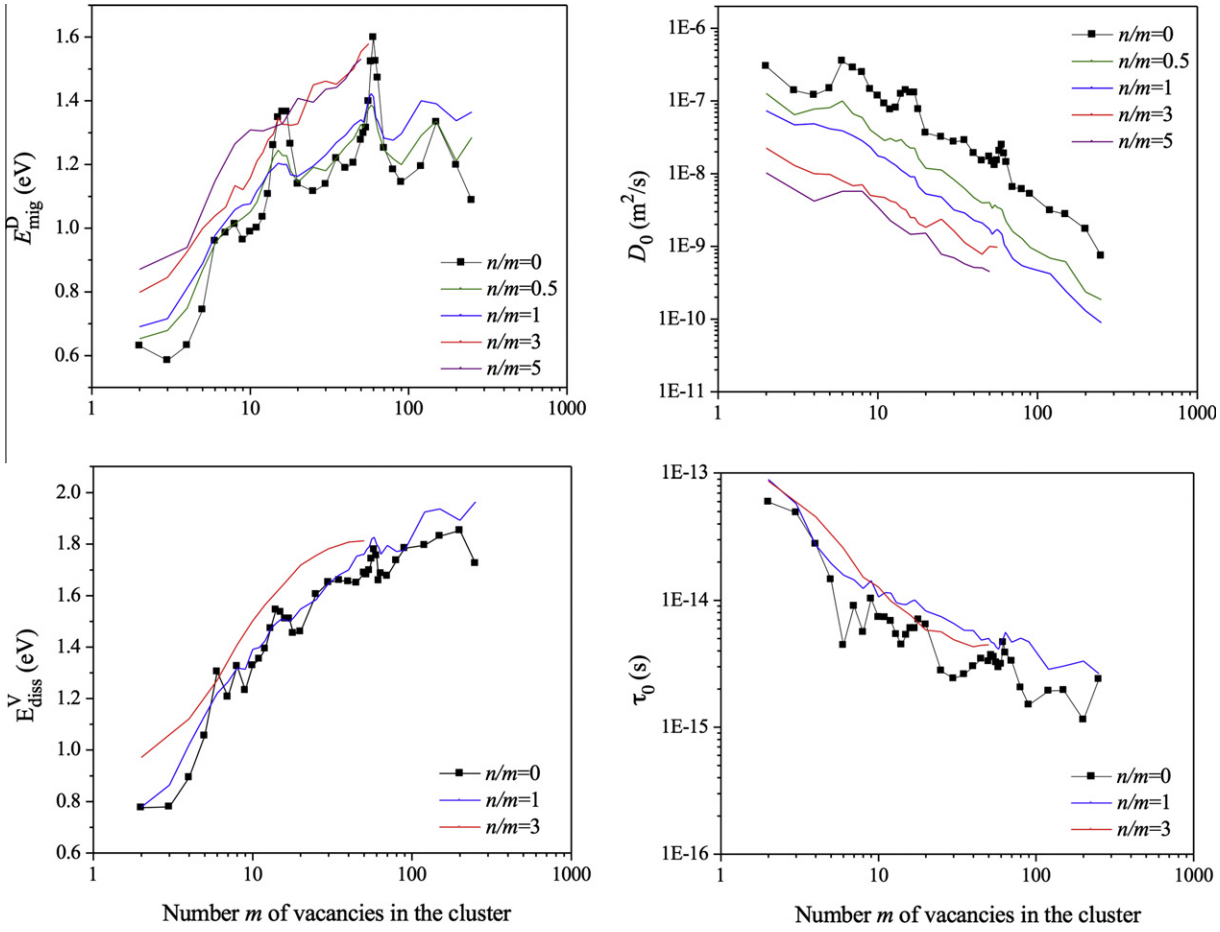

Fig. 7. Evolution with the number m of vacancies in the cluster of the fitted E^D_{mig}, D_0, E^V_{diss} and τ_0 from Eqs. (5) and (6), for different numbers m of Cu atoms in the cluster (thinly coated clusters).

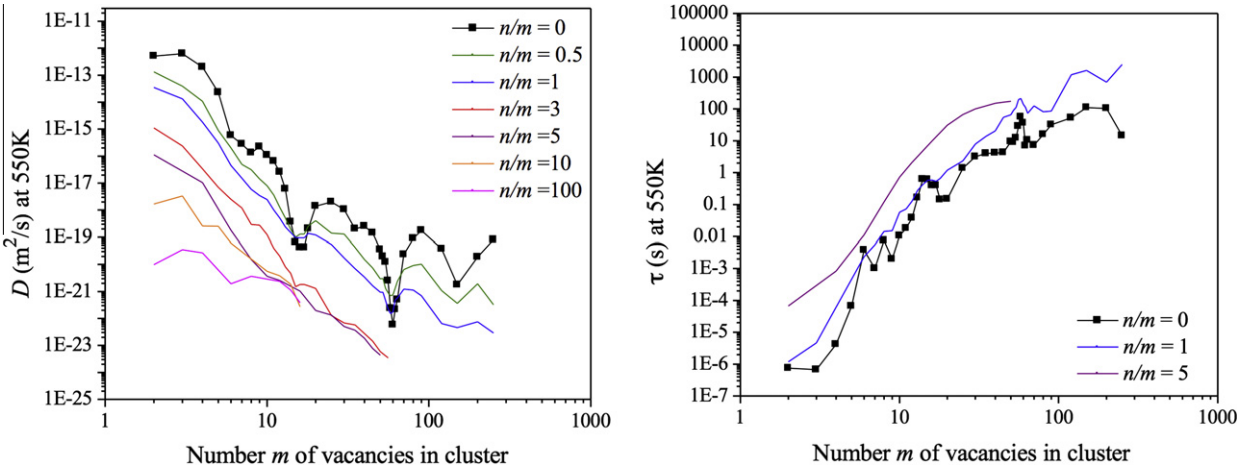

Fig. 8. Evolution with the number m of vacancies in the cluster of D and τ at 550 K, for different numbers n of Cu atoms in the cluster. Values have been calculated using Eqs. (5) and (6), using the coefficients in Fig. 7.

Note that both Al-Motasem et al. [25] and Kulikov et al. [24] showed that Cu coating can be inhomogeneous in some cases, with the outer Cu crown non-concentric with the inner vacancy core. However, for simplicity we initially created all clusters without accounting for this information, thereby letting the algorithm itself lead the system to the most favourable atomic distribution and allow its migration as a consequence of 1nn vacancy jumps, at a given temperature. The simulation is stopped when the cluster has dissociated, i.e. when a vacancy escaped from it and migrated significantly far away from it. Repeating this simulation a large number of times, N^{sim}, enough statistics can be collected to calculate the diffusion coefficients and to estimate the lifetime of each cluster, for a given temperature, following the methodology already applied in [22], i.e. using the following equation:

$$D(T) = \frac{1}{N^{\text{sim}}} \sum_{i=1}^{N^{\text{sim}}} \frac{R_i^2}{6\tau_{\text{life}}^i}(T) \tag{4}$$

where R_i^2 is the square of the total displacement of the centre of mass of the cluster in simulation i, during its lifetime τ_{life}^i in the same simulation. τ_{life} (T) is obtained as average of the different τ_{life}^i .

The temperatures at which Cu precipitation should be studied in connection with RPV steel embrittlement are 290 °C (563 K) for pressurized water reactors, and 265 °C (538 K) in the case of boiling water reactors. In principle, AKMC simulations could be performed directly and only at the desired temperature. It is difficult, though, to achieve sufficient statistics and therefore accuracy in this way, especially for the biggest clusters, because of the strong binding between vacancies and Cu atoms, as already debated in Ref. [30]. The best way to proceed is thus by calculating D and τ_{life} at higher temperatures, and then extrapolate to the desired temperature using Arrhenius functions:

$$D(m,n,T) = D_0(m,n) \cdot \exp(E^D_{\text{mig}}(m,n)/k_BT) \tag{5}$$

$$\tau_{\text{life}}(m,n,T) = \tau_0(m,n) \cdot \exp(E^{-V}_{\text{diss}}(m,n)/k_BT) \tag{6}$$

where the pre-factors D_0 and τ_0, the migration energy E^D_{mig} and the dissociation energy E^{-V}_{diss} are coefficients fitted with a linear regression in an Arrhenius plot ($\ln(D)$ versus $1/k_BT$). This way of proceeding has two advantages. Firstly, high temperatures make the lifetime, and therefore the simulation time, shorter, thereby enabling the collection of much more statistics. Since the model does not allow phase change to fcc or melting and the migration energy is temperature independent by definition, there is no real danger of seeing new phases appear at high temperature, so this procedure is numerically appropriate, even though the temperatures chosen can be physically meaningless (above the temperature where the bcc phase becomes unstable or even above melting temperature). There is, however, a risk of activating new migration and/or dissociation mechanisms, especially for clusters containing many vacancies coated by many Cu atoms, if the temperature is high enough to make the dissociation of the inner vacancy core unstable and dissociate into a collection of single vacancies. Secondly, by studying the process in a wide enough range of temperature any change in the migration mechanism can be detected by non-linearity in the Arrhenius plot: the points sampled in the low temperature range, at the price of a long computing time, are thus used to validate the extrapolations performed from higher temperatures.

Overall we performed 500 AKMC simulations at 11 temperatures that are roughly equidistant on the reciprocal temperature ($1/k_BT$) axis between 2500 K and 550 K, obtaining D and τ_{life} for a wide variety of V_mCu_n clusters: $m = 2,\ldots,250$ and $n/m = 0,1/4,\ 1/2,\ 1,\ 3,\ 5,\ 10,\ 100$. For every cluster, there is a temperature below which the number of AKMC events required to observe its dissociation increases so much that it becomes computationally prohibitive: this temperature is around 650 K for the smallest clusters, up to 900 K for the biggest ones. In these cases, the AKMC simulations were run up to $\sim 10^9$ events: by following the evolution with time of the centre of mass of the cluster, D could still be calculated; but the lifetime τ_{life} could not.

The results we obtained are described and discussed in the two following sections, differentiating between vacancy clusters with thin Cu coating (including cases where the coverage is not complete), and those with thick Cu coating, i.e. Cu precipitates with an inner vacancy core that does not have any contact with the Fe atoms. The reason to separate these two cases is that the physical behaviour is significantly different.

3.2. Vacancy clusters with thin Cu coating

In this section, we consider V_mCu_n clusters that are coated with a thin layer of Cu atoms, or not completely coated. If we consider coating to be complete when the last layer of Cu atoms covers the surface of the vacancy cluster up to the 2nn distance, in a bcc crystallographic structure this corresponds to $n/m \leqslant \sim 2$ for $m \leqslant 100$, and $n/m \leqslant \sim 1$ for $100 < m \leqslant 250$. We thus consider clusters with $n/m \leqslant 5$. The calculated D and τ_{life} show perfect linear trends in Arrhenius plots, thereby suggesting that migration and dissociation mechanisms do not change with temperature.

Fitted coefficients from Eqs. (5) and (6), i.e. migration and dissociation energy, as well as pre-factors, are shown in Fig. 7 as functions of the m/n ratio. Values of diffusion coefficients and lifetimes at 550 K are shown in Fig. 8. We see that, as a general trend, the diffusion coefficient D always decreases when the cluster grows (larger n or m), and the lifetime τ_{life} increases. This is the

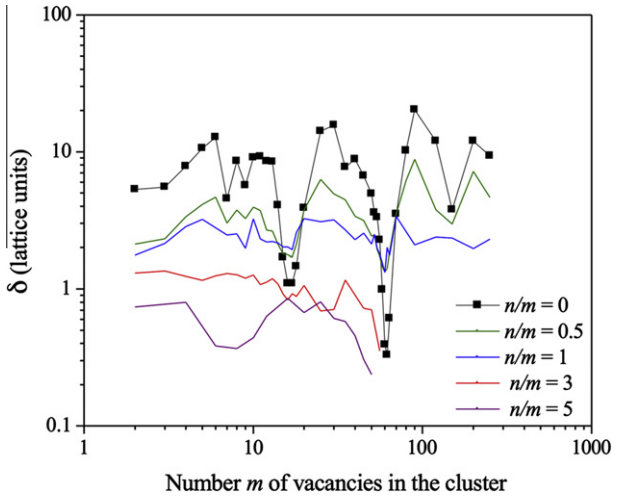

Fig. 9. Evolution with the number m of vacancies in the cluster of the mean free path δ before dissociation (Eq. (7)).

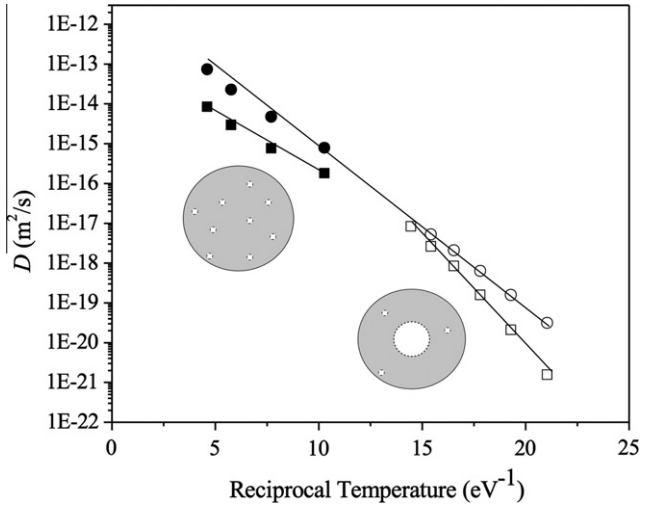

Fig. 10. Examples of Arrhenius plots for the diffusion coefficient. Points are values calculated with AKMC: circles show values for a V_4Cu_{400} cluster, and squares for a $V_{14}Cu_{1400}$ cluster. Lines are fitted expressions using Eq. (5). At low temperature, the vacancies form a stable cluster inside the bulk of Cu. Only a few vacancies escape, and make the whole cluster migrate, by hopping at the Fe–Cu interface. At higher temperatures, the vacancy cluster is completely dissolved in the bulk of Cu, so diffusion becomes more efficient.

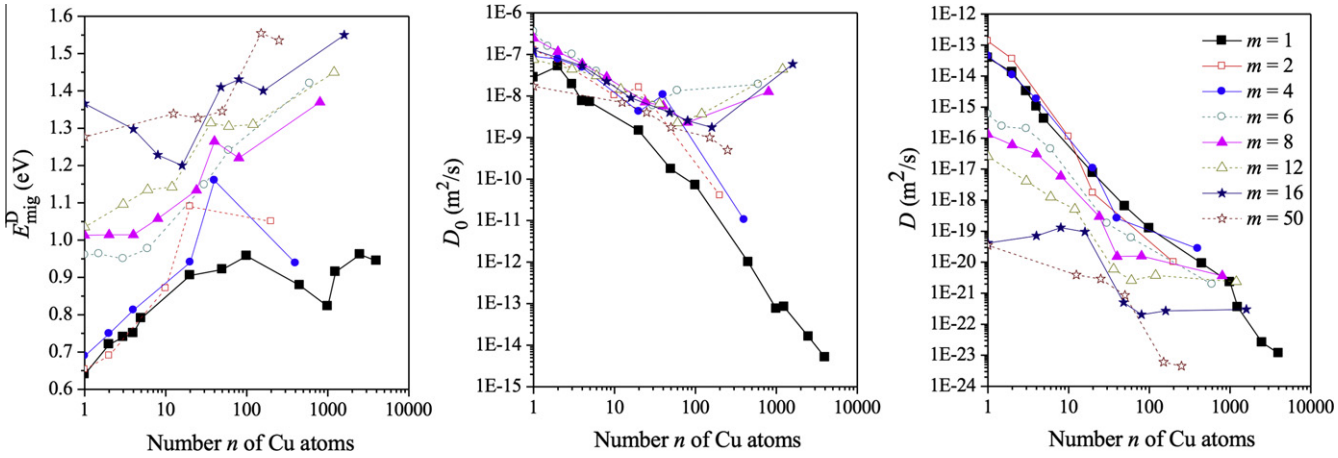

Fig. 11. Evolution with the number n of Cu atoms, for different numbers m of vacancies, of: (left) the migration energy E^D_{mig}; (centre) the diffusion coefficient pre-factor D_0; (right) diffusion coefficient at 550 K. Values for $m = 1$ are taken from Refs. [22], [30].

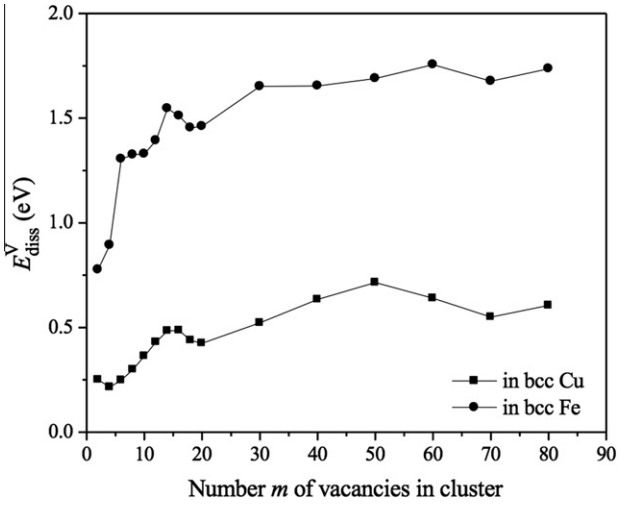

Fig. 12. Dissociation energies E^V_{diss} of V_m clusters in bcc Cu, fitted using Eq. (6) from AKMC data at low temperature, as compared to the same energy in bcc Fe.

natural consequence of the strong binding between vacancies and Cu. The scaling however is not smooth and special configurations with specific "magic" numbers m of vacancies with decreased mobility and increased stability are found: the corresponding D and τ_{life} deviate from the trend by several orders of magnitudes. Those "magic" numbers indeed correspond to particularly stable configurations, in which shells of close neighbours around a central vacancy are completely filled: the 1nn shell for $m = 9$, the 2nn shell for $m = 15$, the 5nn shell for $m = 59$, and the 9nn shell for $m = 137$. The magnitude of the deviation from the trend is progressively damped if the Cu coating increases.

We can deduce from the obtained data the mean free path δ of the clusters, i.e. the average distance they travel before dissociation:

$$\delta = \sqrt{6D\tau} \tag{7}$$

Values at 550 K are shown in Fig. 9. We see that vacancy clusters with incomplete or very thin Cu coatings migrate without dissociation up to relatively large distances. The mean free path rapidly decreases, however, when the Cu coating becomes thicker.

To conclude this section, our results show that vacancy clusters coated with a thin layer of Cu atoms largely behave like pure vacancy clusters, dragging their Cu coating along (which explains why the migration and dissociation mechanism did not change significantly in the large range of temperatures we considered). They can therefore potentially play an important role in the process of Cu precipitation under irradiation, due to their large mobility, because of their ability to drag away a few Cu atoms to distances as large as a few lattice units.

3.3. Vacancy clusters with thick Cu coating

In this section, we consider V_mCu_n clusters that are coated with a thick layer of Cu atoms: $n/m = 10$ and 100, i.e. clusters that can be defined as hollow precipitates, with an inner core of vacancies not in contact with Fe atoms (in their most stable configuration). Differently from thinly coated clusters, here a significant change in the diffusion and dissociation mechanisms versus temperature is observed, as illustrated in Fig. 10. This change has its origin in the fact that above a certain temperature the inner vacancy core becomes unstable and is replaced by a collection of single vacancies migrating inside the precipitate and sometimes reaching the interface with Fe atoms, thereby allowing rapid migration. Below this temperature, on the contrary, the vacancy core evolves remaining inside the precipitates, making the diffusion of the cluster as a whole extremely inefficient. In the lower temperature range vacancy emission from the cluster never occurs (within reasonable simulation times). As a consequence, no cluster lifetime can be estimated in this range and any extrapolation to around 550 K from values calculated at high temperature would underestimate it by many orders of magnitudes.

Migration and dissociation energy, as well as pre-factors, fitted from Eqs. (5) and (6) in the low temperature range, are shown in Fig. 11. Results obtained in the previous section were also included in the figure to look at their global evolution with the number n of Cu atoms in the cluster. Comparison is performed with clusters containing a single vacancy. We see that V_mCu_n clusters can be classified in two groups. In the first group, $m < 6$, clusters behave apparently in a similar way as clusters with one vacancy: from a certain m, the migration energy saturates, and the pre-factor D_0 decreases by several orders of magnitudes. This indicates that vacancies are trapped inside the bulk of the Cu cluster, whose volume increases, and have therefore less opportunity to hop at the Fe–Cu interface. The surface of the latter, with increasing m, is more and more regular, and its curvature remains almost identical: this explains why the cluster migration energy remains nearly constant. In the second group, $m \geqslant 6$, the coefficients follow a significantly different evolution: from a certain m, the migration energy

increases substantially, while the pre-factor slightly increases. This suggests that the cluster behaviour is, in this case, dictated by the increasing stability of the inner core of vacancies. The Fe–Cu interface being essentially insensible to the number of vacancies (Cu coating is thick enough), only a large increase of the stability of the vacancy core can explain the large increase of the cluster migration energy. The increase of the pre-factor is then merely a numerical effect. To check this statement, we have calculated the dissociation energy of vacancy clusters in bcc Cu, as shown in Fig. 12 and compared with the same energy in bcc Fe. AKMC simulations are, in this case, relatively fast, and the lifetime can be calculated even at low temperature. We see that the dissociation energy substantially increases with m, in agreement with our conclusion, while being much smaller than in Fe, thereby explaining the fact that thinly coated vacancy clusters in Fe have much longer lifetimes. The important consequence of these results is that there is no reason to expect big Cu clusters to become significantly more mobile if more than $\sim$16 vacancies are added, i.e. the diffusion coefficient decreases instead of further increasing.

This is clearly shown in the right part of Fig. 11, where the values of D at 550 K are indicated. It is also interesting to observe that the mobility of Cu clusters is almost never improved if they contain more than one vacancy. Deviations from $m = 1$ are especially large (by several orders of magnitude) for the smallest clusters, i.e. for the most mobile ones. For the largest Cu clusters, on the contrary, diffusion coefficients are less sensitive to the number of vacancies, as well as to the number of Cu atoms.

4. Conclusive remarks

We have calculated the diffusion coefficient and lifetime of vacancy–copper clusters, in a large variety of sizes and compositions, using a fully atomistic model with limited and reasonable approximations and simplifications about the migration and dissociation mechanisms, as they spontaneously take place as a consequence of elementary migration events (single vacancies of the cluster to a 1nn position). The only physical input of the model is the interatomic potential by Pasianot et al. [54], which has already been shown to predict the correct kinetics of precipitation [30]. The numbers obtained here can be used as input data for coarse-grained models such as object kinetic Monte Carlo, to simulate radiation-enhanced precipitation in Fe–Cu alloys, as model systems for RPV steels.

The main reason that motivated us to perform this work is the fact that the mechanism under which Cu precipitates in Fe during thermal annealing is driven by the mobility of Cu clusters, because of the vacancy hops at their surface, as demonstrated in [30]. Our results reveal that, contrary to what intuition might firstly suggest, the mobility of Cu precipitates under irradiation is *reduced* by the presence of a large amount vacancies inside. As a consequence, the rate of Cu precipitate coarsening under irradiation is expected to be also reduced and this might partly explain why under irradiation copper precipitation takes the form of a large density ($\sim 10^{24}\,\mathrm{m}^{-3}$) of small-size (2–4 nm) clusters in Fe–Cu alloys [8,59], as opposed to large precipitates produced after annealing. Of course, only the implementation of the data we calculated in this work in appropriate OKMC or equivalent models can provide a full confirmation to this surmise. This will be the subject of future work.

Acknowledgements

This research has received partial funding from the European Atomic Energy Community's 7th Framework Program (FP7/2007-2011), under Grant Agreement Number 232612 (Perform60 project).

The work was also partially sponsored by the belgo-argentine FWO–MINCyT bilateral cooperation agreement, Project VS. 004.10N.

References

[1] G.R. Odette, G.E. Lucas, JOM 53 (7) (2001) 18–22.
[2] U. Potapovs, J.R. Hawthorne, Nucl. Appl. 6 (27) (1969).
[3] G.R. Odette, Scripta Metall. 17 (1983) 1183.
[4] J.T. Buswell, C.A. English, M.G. Hetherington, W.J. Phythian, G.D.W. Smith, G.M. Worrall, Effects of radiation on materials, in: N.H. Packan, R.E. Stoller, A.S. Kumar (Eds.), 14th International Symposium (Vol. II), ASTM STP 1046, American Society for Testing and Materials, Philadelphia, 1990 pp. 127–153.
[5] W.J. Phythian, A.J.E. Foreman, C.A. English, J.T. Buswell, M. Hetherington, K. Roberts, S. Pizzini, Effects of radiation on materials, in: R.E. Stoller, A.S. Kumar, D.S. Gelles (EDs.), 15th International Symposium, ASTM STP 1125, American Society for Testing and Materials, Philadelphia, 1992, pp. 131–150.
[6] T.N. Lê, A. Barbu, D. Liu, F. Maury, Scripta. Metall. Mater. 26 (1992) 771.
[7] J.T. Buswell, W.J. Phythian, R.J. McElroy, S. Dumbill, P.H.N. Ray, J. Mace, R.N. Sinclair, J. Nucl. Mater. 225 (1995) 196.
[8] P. Auger, P. Pareige, S. Welzel, J. Nucl. Mater. 280 (2000) 331.
[9] S.I. Golubov, Y.N. Osetsky, A. Serra, A.V. Barashev, J. Nucl. Mater. 226 (1995) 252.
[10] S.I. Golubov, A. Serra, Y.N. Osetsky, A.V. Barashev, J. Nucl. Mater. 277 (2000) 113.
[11] F. Christien, A. Barbu, J. Nucl. Mater. 324 (2004) 90.
[12] A. Barashev, S. Golubov, D. Bacon, P. Flewitt, T. Lewis, Acta Mater. 52 (2004) 877.
[13] L. Malerba, C.S. Becquart, M. Hou, C. Domain, Phil. Mag. 85 (2003) 417.
[14] C.S. Becquart et al., J. nucl. Mater. 406 (2010) 39.
[15] C. Domain, C.S. Becquart, Phys. Rev. B 65 (2001) 024103.
[16] C.S. Becquart, C. Domain, Nucl. Instrum. Methods. B 202 (2003) 44.
[17] G. Brauer, K. Popp, Phys. Status Solidi 102 (1987) 79.
[18] A. Möslang, E. Albert, E. Recknagel, A. Weidinger, P. Moser, Hyperfine Interact. 15 (1983) 409.
[19] A. Arokiam, A. Barashev, D. Bacon, Y. Osetsky, Philos. Mag. Lett. 85 (2005) 491.
[20] A.V. Barashev, A.C. Arokiam, Philos. Mag. Lett. 86 (2006) 321.
[21] F. Soisson, C.C. Fu, Solid State Phenom. 139 (2008) 107.
[22] M.I. Pascuet, N. Castin, C.S. Becquart, L. Malerba, J. Nucl. Mater. 412 (2011) 106.
[23] F. Soisson, C.C. Fu, Phys. Rev. B 76 (2007) 214102.
[24] D. Kulikov, L. Malerba, M. Hou, Philos. Mag. 86 (2006) 141.
[25] A.T. Al-Motasem, M. Posselt, F. Bergner, U. Birkenheuer, J. Nucl. Mater. 414 (2011) 161.
[26] Y. Nagai, Z. Tang, M. Hassegawa, T. Kanai, M. Saneyasu, Phys. Rev. B 63 (2001) 134110.
[27] Y. Nagai, K. Takadate, Z. Tang, H. Ohkubo, H. Sunaga, H. Takizawa, M. Hasegawa, Phys. Rev. B 67 (2003) 224202.
[28] E. Meslin et al., J. Nucl. Mater. 406 (2010) 73.
[29] M. Lambrecht, E. Meslin, L. Malerba, M. Hernandez-Mayoral, F. Bergner, P. Pareige, B. Radiguet, A. Almazouzi, J. Nucl. Mater. 406 (2010) 84.
[30] N. Castin, M.I. Pascuet, L. Malerba, J. Chem. Phys. 135 (2011) 064502.
[31] N. Castin, L. Malerba, J. Chem. Phys. 132 (2010) 074507.
[32] S.R. Goodman, S.S. Brenner, J.R. Low, Metall. Trans. 4 (1973) 2363.
[33] R. Kampmann, R. Wagner, in: C. Janot, W. Petry, D. Richter, T. Springer (Eds.), Atomic Transport and Defects in Metals by Neutron Scatterings, Springer, New York, 1986, p. 73.
[34] M.H. Mathon, A. Barbu, F. Dunstetter, F. Maury, N. Lorenzelli, C.H. De Novion, J. Nucl. Mater. 245 (1997) 224.
[35] M. Perez, F. Perrard, V. Massardier, et al., Philos. Mag. 85 (2005) 2197.
[36] E. Vincent, C.S. Becquart, C. Pareige, P. Pareige, C. Domain, J. Nucl. Mater. 373 (2008) 387.
[37] A. Deschamps, C. Genevois, M. Nicolas, F. Perrard, F. Bley, Philos. Mag. 85 (2005) 3091.
[38] F. Soisson, A. Barbu, G. Martin, Acta Mater. 44 (1996) 3789.
[39] S. Schmauder, P. Binkele, Comput. Mater. Sci. 25 (2002) 174.
[40] W.M. Young, E.W. Elcock, Proc. Phys. Soc. 89 (1966) 735.
[41] B. Bortz, M.H. Kalos, J.L. Lebowitz, J. Comput. Phys. 17 (1975) 10.
[42] K.A. Fichthorn, W.H. Weinberg, J. Chem. Phys. 95 (1991) 1090.
[43] C.S. Becquart, C. Domain, Phys. Status Solidi b 247 (2010) 9.
[44] P. Bellon, Microst. Plasticity 108 (2003) 395. References therein.
[45] Y. Le Bouar, F. Soisson, Phys. Rev. B 65 (2002) 094103.
[46] J.M. Sanchez, F. Ducastelle, D. Gratias, Phys. A 128 (1984) 334.
[47] A. Van der Ven, G. Ceder, M. Asta, P.D. Tepesch, Phys. Rev. B (2001) 64.
[48] K. Sastry, D.D. Johnson, D.E. Goldberg, P. Bellon, Phys. Rev. B 72 (2005) 085438.
[49] G. Bonny, D. Terentyev, L. Malerba, Comput. Mater. Sci. 42 (2008) 107.
[50] G. Bonny, D. Terentyev, L. Malerba, D. Van Neck, Phys. Rev. B 79 (2009) 104207.
[51] F. Soisson, C.S. Becquart, N. Castin, C. Domain, L. Malerba, E. Vincent, J. Nucl. Mater. 406 (2010) 55.
[52] E. Vincent, C.S. Becquart, C. Domain, Nucl. Instr. Meth. Phys. Res. B 255 (2007) 78.
[53] E. Vincent, C.S. Becquart, C. Domain, J. Nucl. Mater. 382 (2008) 154.
[54] R.C. Pasianot, L. Malerba, J. Nucl. Mater. 360 (2007) 118.
[55] M. Talati, M. Posselt, G. Bonny, A.T. Al-Motasem, F. Bergner, J. Phys. Cond. Mater. 24 (2012) 225402.

[56] V.P. Ramunni, M.A. Alurralde, R.C. Pasianot, Phys. Rev. B 74 (2006) 054113.
[57] G. Henkelman, H. Jónsson, J. Chem. Phys. 111 (1999) 7010.
[58] C. Domain, C.S. Becquart, L. Malerba, J. Nucl. Mater. 335 (2004) 121.
[59] M.K. Miller, K.F. Russell, J. Nucl. Mater. 371 (2007) 145.